

THE NUMERICAL MODELLING OF LONG WAVE PROPAGATION IN THE FRAMEWORK OF NON-LINEAR DISPERSION MODELS

L. B. CHUBAROV and YU. I. SHOKIN†

Computing Center of Siberian Division of the U.S.S.R., Academy of Sciences, 660036,
Krasnoyarsk 36, Akademgorodok, U.S.S.R.

(Received 22 January 1986)

Abstract—The work is devoted to the questions of numerical modelling of long wave propagation, in particular tsunami waves, in the framework of non-linear dispersion models of the Boussinesq and Korteweg-de Vries type.

The first part of the work includes a classification of some known mathematical models, in terms of dispersion correlation, phase and group velocities.

Problems arising on the construction of finite-difference approximations of non-linear dispersion models are discussed in the second part of the work, special attention is given to the questions of constructing discrete boundary conditions.

In conclusion the results obtained in the course of numerical experiments and estimation of specifics of finite-difference models, and the contribution of non-linear dispersion effects in the process of wave propagation in the coastal zone, are discussed. The results of calculations of tsunami wave propagation in a wave tube with real bathymetry, are given.

1. INTRODUCTION

Consider an ideal incompressible liquid in the homogeneous field of gravitational forces. Assume the flow to be potential, i.e. for the velocity vector $\mathbf{u} = \{u, v, w\}$ there exists the function $\phi(x, y, z, t)$ so that $\mathbf{u} = \text{grad } \phi$. Here u, v, w are the components of the velocity vector along the axis x, y, z , respectively, the axis z being directed vertically upward—opposite to the direction of the free fall acceleration.

An introduction, according to the monograph [1], to a number of notions necessary for further definition.

For a wave we take any discernible signal sent from one part of the medium to another with some velocity, it may be distorted, and alter in quantity and propagation velocity.

Any signal with the Fourier transform (or an integral) may be presented as a superposition of simple waves (harmonics) having this form:

$$\eta = \eta_0 \cos(kx - \omega t), \quad (1)$$

where $\theta = kx - \omega t$ is the phase, k is the wave number, $\omega = \omega(k)$ is frequency and the function $\omega(k)$ is defined by a concrete form of a mathematical model chosen for the investigation of this physical phenomenon.

Waves are called dispersive, if the phase velocity $c_F = \omega(k)/k$ is the function of the wave number: $c_F = c_F(k)$. This means, if the general solution of the problem is the superposition of harmonics then the constituents of the primary signal corresponding to different wave numbers will propagate with different velocities. A particular note should be taken of the situation when the phase velocity depends not only on the wave number but also on the wave amplitude. In this case the so-called non-linear effects are displayed.

Let's introduce to a notion of group velocity $c_G(k) = \partial\omega/\partial k$. It can be shown, that just with this velocity, energy propagates in the wave train which will be referred to as a long oscillating sequence of waves, resulted from dispersion of a primary single signal.

†To whom correspondence should be addressed.

Passing to the consideration of waves on the surface of an ideal incompressible heavy liquid, the simplest linear theory of small amplitude waves [2] leads to the dispersive relation:

$$\omega = \pm \sqrt{gk \operatorname{th}(kD_0)}, \quad (2)$$

where g is the gravity force acceleration, D_0 is the depth of undisturbed liquid. From equation (2) at $kD_0 \rightarrow \infty$ (for deep water or short waves) we have: $\omega = \pm \sqrt{gk}$.

For a solitary wave [3, 4], consisting of one hump and having an infinite period, the form of the free surface and the propagation velocity are described by the expressions:

$$\eta = \eta_0 \operatorname{sech}^2 \left\{ \left(\frac{c_1 \eta_0}{12 \nu} \right)^{1/2} (x - Ut) \right\} \quad (3)$$

$$U = -(c_0 + \frac{1}{3} c_1 \eta_0). \quad (4)$$

The relations (3) and (4) can be obtained directly from the Korteweg-de-Vries equation [5] describing long waves in shallow water:

$$\eta_t + (c_0 + c_1 \eta) \eta_x + \nu \eta_{xxx} = 0, \quad (5)$$

where c_0 , c_1 , ν are constants.

Note, that here we see the above mentioned dependence of the wave propagation velocity, equation (4), on its amplitude η_0 . This dependence is possible only at $c_1 \neq 0$ so that equation (5) can be called the simplest model including non-linear $c_1 \eta \eta_x$ and dispersive $\nu \eta_{xxx}$ members.

The main nondimensional parameters determining the significance of these or other effects, when considering waves on the surface of liquid, usually have the form $\epsilon = \eta_0/D_0$, $\sigma^2 = D_0^2/\lambda^2$, where η_0 , D_0 are the typical wave amplitude and depth of liquid, and λ_0 is the typical wave length. The parameters ϵ and σ^2 have a definite physical sense, for instance, from the dispersive relation equation (2), which is characteristic of linear waves of small amplitude, one can obtain the approximate value of the phase velocity:

$$c_F \sim \sqrt{gD_0} \left(1 - \frac{2\pi^2 \sigma^2}{3} \right). \quad (6)$$

It follows from equation (6) that σ^2 defines the measure of a frequency dispersion. At the same time the propagation velocity of a solitary wave equation (4), whose existence is due to non-linear effects, depends on the parameter ϵ :

$$U \sim c_0 + \frac{1}{3} c_1 \epsilon,$$

i.e. ϵ is the measure of non-linear or amplitude dispersion.

A quantitative union between these two forms of dispersion is established by the Ursell parameter:

$$U = \epsilon/\sigma^2. \quad (7)$$

Thus, at $U \ll 1$ non-linear effects may be neglected and, adversely, at $U \gg 1$ they prove to be determinant. For the Ursell parameter values close to one, the description of a process in terms of mathematical models is natural, which account of both non-linear (amplitude) and frequency dispersion.

In recent years the attention of researchers, concerned with problems of mathematical modelling of tsunami waves, appeared to be drawn to the study of the influence of dispersion effects on characteristics of these waves which, in turn, caused a necessity of constructing new models and more profound analysis of already existing non-linear-dispersion models [6].

A systematic derivation of approximate models from exact equations of hydrodynamics is implemented in the form of constructing sequential approximations. This process consists in a formal expansion of all values into a power series of some small parameter and a subsequent retention of the members of one infinitesimal. The works of

K. Fridrikhse [7], J. Keller [8], M. A. Lavrentyev [4], J. J. Stoker [9], L. V. Ovsyannikov [10] and others are devoted to the problems of substantiation of such an approach.

One of the first non-linear dispersion models was suggested in the paper Ref. [3]. This model describes a wave propagation on the surface of the canal with constant depth. With the development of computational facilities and numerical methods of the solution of mathematical physics non-linear-dispersion models have been introduced for consideration taking into account an arbitrary form of a basin bottom [11–14] and also effects caused by the bottom displacement occurring on the background of a process of the wave propagation [15, 16].

Note, that equations of the Boussinesq–Korteweg-de-Vries type describe a wide range of phenomena occurring in dispersive media, for example, the propagation of temperature waves in plasma etc., but the subject of the present study will be only waves propagating on the surface of an ideal incompressible heavy liquid.

The aim of this work is, firstly, to give a classification of non-linear-dispersion models from the point of view of constructing their finite-difference approximations possessing the properties of efficiency and stability in relation to high frequency perturbations, secondly, to construct and an experimental substantiation of finite-difference algorithms, realizing boundary problems, formulated subject to real situations, arising in the problems on the propagation and transformation of tsunami waves. And third, to study experimentally, with the above mentioned algorithms, of the influence of non-linear and dispersion effects on the characteristics of tsunami waves in the coastal zone.

2. NON-LINEAR DISPERSION MODELS OF WAVE PROPAGATION ON THE WATER

2.1. Differential equations

A variety of non-linear-dispersion models having the same order of a hydrodynamical approximation according to ϵ and σ^2 is accounted for, firstly, by various ways of modifying the dispersive members themselves with the help of relations of the lower order of a hydrodynamical approximation and, secondly, by a wide choice of dependent variables.

Thus, the above Boussinesq’s system of equations [3] has the form:

$$\begin{cases} h_t + (uh)_x = 0, \\ u_t + uu_x + gh_x + \frac{D_0}{3} h_{xxt} = 0. \end{cases} \quad (8)$$

With the help of the relations of the linear theory of shallow water:

$$\begin{cases} u_t + g\eta_x = 0, \\ \eta_t + (D_0 u)_x = 0, \end{cases} \quad (9)$$

from system (8) one can obtain an equivalent system of equations

$$\begin{cases} h_t + (uh)_x = 0, \\ u_t + uu_x + gh_x + \frac{c_0 D_0}{3} h_{xxx} = 0, \end{cases} \quad (10)$$

where $h = D_0 + \eta$ is the full depth of the water, η is the elevation of a free surface over the horizontal level, u is the horizontal local liquid velocity and $c_0 = \sqrt{gD_0}$ is the typical velocity of long waves propagation in shallow water.

Consider an example demonstrating one more possibility of modifying non-linear dispersion models. In paper Ref. [17] is given a system of equations having, in non-dimensional variables, the form:

$$\begin{cases} \eta_t + u_x + \epsilon(u\eta_x - \eta_t + \frac{1}{6}\eta_{ttt}) = 0(\epsilon^2), \\ u_t + \eta_x + \epsilon(-u\eta_t + \frac{1}{2}\eta_{xu}) = 0(\epsilon^2). \end{cases} \quad (11)$$

Here u is the velocity at the bottom of the basin, the depth of which is constant and equals 1.

Equations (11) may be modified either with relations analogous to system (9):

$$\begin{cases} u_t + \eta_x = 0(\epsilon), \\ \eta_t + u_x = 0(\epsilon), \end{cases} \quad (12)$$

or at the expense of introducing the velocity u determined at the height z above the bottom level:

$$u = U - \frac{\epsilon}{2} z^2 U_{xx} + 0(\epsilon^2), \quad 0 \leq z + 1 + \eta,$$

or the velocity v on the free surface:

$$v = U - \frac{\epsilon}{2} (1 + \epsilon\eta)^2 U_{xx} + 0(\epsilon^2),$$

or the velocity w determined from the kinetic energy flow:

$$\left(\int_0^{1+\epsilon\eta} w^3 dz \right)^{1/3} = U + \epsilon \left(\frac{1}{3} U_\eta - \frac{1}{6} U_{xx} \right) + 0(\epsilon^2).$$

Let's introduce some auxiliary notations. By the vector $\mathbf{u} = \{u, v\}$ we mean a vector whose components are projections on horizontal axes of the system of coordinates, the operators $\text{div}(\)$, $\text{grad}(\)$ here and below will be treated as operators acting in the horizontal plane:

$$\text{div } \mathbf{u} = u_x + v_y, \quad \text{grad } f = f_x \mathbf{i}_x + f_y \mathbf{i}_y,$$

where $\mathbf{i}_x, \mathbf{i}_y$ are the single unit vectors of the axes OX and OY .

Now we pass to the consideration of non-linear dispersion models describing the wave propagation in a two-level basin with an arbitrary relief of the bottom.

At the beginning of this trend investigations [11] were carried out in which the following equations are suggested:

$$\begin{cases} \mathbf{u}_t + \mathbf{u} \text{ grad } \mathbf{u} + \mathbf{g} \text{ grad } \eta = \frac{1}{2} D \left\{ \text{grad}[\text{div}(D\mathbf{u})] - \frac{D}{6} \text{grad div } \mathbf{u} \right\}_t, \\ \eta_t + \text{div}\{(D + \eta)\mathbf{u}\} = 0, \end{cases} \quad (13)$$

$$\begin{cases} \mathbf{u}_t + \mathbf{u} \text{ grad } \mathbf{u} + \mathbf{g} \text{ grad } \eta = 0, \\ \eta_t + \text{div}\{(D + \eta)\mathbf{u}\} + \frac{1}{2} \text{div} \left\{ D^2 \text{grad}[\text{div}(D\mathbf{u})] - \frac{D^3}{3} \text{grad div } \mathbf{u} \right\} = 0. \end{cases} \quad (14)$$

In equations (13) and (14) the vector \mathbf{u} is the velocity flow-averaged, and the velocity on the horizontal plane $z = 0$, respectively; the function D describes the distribution of the basin depths: $z = -D(x, y)$.

Non-linear dispersion models accounting of the bottom displacement effects were suggested in Ref. [16]. In this work the authors introduce a small parameter $\mu = W/\sqrt{gD_0}$, (where W is the value characterizing the bottom displacement velocity) and the parameter σ preserves its sense. On deriving equations, it is considered that $\sigma^2 \sim \mu$ and the members having the order of infinitesimals $0(\mu, \sigma^2)$ are retained. Then, in terms of velocity on the horizontal plane $z = 0$:

$$\begin{aligned} \mathbf{u}_t + \mathbf{u} \text{ grad } \mathbf{u} + \mathbf{g} \text{ grad } \eta + \text{grad}(DR_{tt}) &= \frac{1}{2} \text{grad div}(D^2 \mathbf{u}_t), \\ \eta_t + \text{div}[(D + \eta - R)\mathbf{u}] + \frac{1}{2} \text{div grad}(D^2 R_t) &= \frac{1}{2} \text{div}[\text{grad div}(D^3 \mathbf{u})], \end{aligned} \quad (15)$$

and in terms of the flow-averaged velocity:

$$\begin{aligned} \mathbf{u}_t + \mathbf{u} \operatorname{grad} \mathbf{u} + \mathbf{g} \operatorname{grad} \eta + \frac{1}{2} \operatorname{grad}(D R_{tt}) &= \operatorname{grad} \left(\frac{D^2}{3} (\operatorname{div} \mathbf{u})_t + \frac{D}{2} \operatorname{grad} D \mathbf{u}_t \right), \\ \eta_t + \operatorname{div}[(D - \eta + R) \mathbf{u}] + \frac{1}{2} \operatorname{div}[D \operatorname{grad}(D R_{tt})] &= \frac{1}{6} \operatorname{div}[3D (\operatorname{grad} D^2) \mathbf{u} + D^2 \operatorname{grad}(D \operatorname{div} \mathbf{u})] \end{aligned} \quad (16)$$

In equations (15) and (16) $R = R(x, y, t)$ is the function describing the change of the basin depth. Note, that at $R \equiv 0$ equations (16) go over into the relations considered in Ref. [13], and equation (15) at $D \equiv \text{constant}$ into the relations studied in Ref [15].

It is necessary to emphasize that the models (15) and (16) allow one to study processes of a tsunami wave generation with the account of dispersive properties of the liquid.

To conclude this point, we mention a non-linear dispersion model constructed by the authors of a previous paper [18] and having a special form convenient for a numerical approximation by the method of characteristics [25].

Let us go back to system (8) and consider its linearization on the solution of the form:

$$u = u_0 + \tilde{u}, \quad h = D_0 + \eta, \quad D_0 \equiv \text{constant}, \quad u_0 \equiv \text{constant}, \quad (17)$$

here we shall presuppose the infinitesimal of the product of the values \tilde{u} and η and also their first derivatives. The result of such a transformation will be the system:

$$\begin{cases} \eta_t + D_0 \tilde{u}_x + u_0 \eta_x = 0, \\ \tilde{u}_t + u_0 \tilde{u}_x + g \eta_x = 0, \end{cases} \quad (18)$$

which can be reduced to one equation:

$$\eta_{tt} + 2u_0 \eta_{xt} + (u_0^2 - c_0^2) \eta_{xx} = \frac{D_0^2}{3} \eta_{xxx}. \quad (19)$$

At small velocities ($u_0^2 < c_0^2$), equation (19) is a wave equation with a dispersive addition. This equation may serve as a simple model for the study of dispersion properties of the initial system (8). A study of non-linear effects turns out to be impossible here due to linearization in going from equation (8) to equation (18).

Consider the solution of equation (19) of a progressing wave type:

$$\eta = \exp\{i(kx - \omega t)\}, \quad (20)$$

its frequency is connected with a wave number by the dispersion relation

$$\omega^2 \left(1 + \frac{D_0^2 k^2}{3} \right) - 2u_0 k \omega + (u_0^2 - c_0^2) k^2 = 0. \quad (21)$$

Where:

$$\omega_{1,2} = \frac{u_0 k \pm \sqrt{c_0^2 - (u_0^2 - c_0^2)(1 + D_0^2 k^2/3)}}{1 + D_0^2 k^2/3}. \quad (22)$$

It follows from equation (22), that at $u_0^2 < c_0^2$ for all the wave numbers frequencies are in the real range and the solution of the equation (20) will be stable, while at $u_0^2 > c_0^2$ for sufficiently large k the frequencies ω become imaginary, which may result in the development of instability. We shall conduct further consideration at the following simplifying assumption:

$$u_0 \equiv 0,$$

in this case from equation (21) follows:

$$\omega^2 = c_0^2 k^2 / (1 + D_0^2 k^2/3). \quad (23)$$

For tsunami waves the accepted simplifying assumption is quite possible, as $c_0^2 = g D_0$, where D_0 is the ocean depth, while u is the local average velocity of liquid particles, which is a small value.

Having made analogous transformations for system (10) we arrive at the analogue of relation (23):

$$\omega^2 = c_0^2 k^2 - \frac{1}{3} c_0^2 D_0^2 k^4. \quad (24)$$

As it was noted in Ref. [1], expansions (23) and (24) in terms of the small parameter $(kD_0)^2$ agree with an accuracy up to the second order members and, therefore, systems (8) and (10) are equivalent in this approximation. However, with increasing the parameter $\sigma^2 \sim k^2 D_0^2$ solutions of system (10), containing high-frequency components, now become unstable at any relations of the velocities u_0, c_0 , since at large k the frequency ω goes over into the imaginary field.

The analogue of relation (23), derived under the same assumptions and by the same procedure as equation (23), here and below will be referred to as the dispersion relation of the system.

Consider the system of equations suggested by L. V. Ovsyannikov [10]:

$$\begin{cases} h_t + (hu)_x + \frac{1}{3}(hu_x)_{xx} = 0, \\ u_t + (u^2/2 + gh)_x - \frac{1}{2}(h^2 u_{xx})_x = 0, \end{cases}$$

its dispersion relation coincides with equation (24), and the system, transformed by equation (9), will possess dispersion relation (23).

The main result of this paragraph, a classification of some non-linear dispersion models, will now be considered. We shall assume, that each of the considered systems of equations was subjected to the procedure, described in the foregoing point, as a result, a dispersion relation was derived, from which phase and group velocities were determined. We can assume, that the limits of these velocities are equal to zero at large k and we will favour the results of numerical calculations made by the models having such a property. Essentially, it means that high-frequency harmonics, inevitably emerging, when setting initial and boundary conditions, and also in the process of rounding-off, will have a weak influence on the character of the solution. This property appears to be related with the stability of solutions of differential models, and namely with the transition of values of ω frequencies from the real region to the imaginary one, following from dispersion relations. The results of the classification are tabulated, so that the following notations are introduced:

$$\begin{aligned} L_{10}(\phi, \psi) &= \phi_t + (\phi\psi)_x; & L_{11}(\phi, \psi) &= \phi_t + \psi_x; \\ L_{20}(\phi, \psi) &= \psi_t + \frac{1}{2}(\psi^2)_x + g\phi_x; \\ L_{21}(\phi, \psi) &= \psi_t + \phi_x; & c_F &= \omega/k; & c_G &= d\omega/dk; & c_{F_\infty} &= \lim_{|k| \rightarrow \infty} c_F; & c_{G_\infty} &= \lim_{|k| \rightarrow \infty} c_G. \end{aligned}$$

From the considered models the ones, denoted by us, (A, C, D, H, K) possess the property of the values c_{F_∞} and c_{G_∞} being equal to zero. The models (F, G) adjoin them, for which the values c_{F_∞} and c_{G_∞} are finite, and the corresponding frequencies ω_F and ω_G are real. Note, that with a numerical realization of these models it is obligatory to use either implicit or multi-level explicit finite difference schemes due to the presence of dispersive members with mixed (spatial-time) derivatives. At the same processes connected with tsunami wave propagation are "rapid", i.e. they are characterized by high velocities and small typical time characteristics, so that the main merits of implicit difference schemes, allowing big steps in time, prove to be inapplicable. We are interested in the solution of problems in the areas with inner boundaries of a complex configuration, so that it is desirable to preserve the possibility of applying two-level explicit finite difference schemes, making the algorithm more flexible and simple. This is possible in the framework of models of the B, L type, however, their intrinsic dispersion relations indicate an unlimited growth of high-frequency harmonics. This sets extra limitations on numerical algorithms and requires a strong suppression of high-frequency components in going from one time level to another, to realize these models.

Somewhat different from the others is the model E , which possesses finite, but not

Table 1

Index	Phase velocity	c_{ps}	Group velocities	c_{po}	Equations	References
A	$\pm c \left(1 + \frac{H_0^2 k^2}{3}\right)^{-3/2}$	0	$\pm c \left(1 + \frac{H_0^2 k^2}{3}\right)^{-1/2}$	0	$L_{10}(h, u) = 0, \quad L_{20}(h, u) = -\frac{H_0}{3} h_{,xx}$	J. Boussinesq [3]
B	$\pm c \left(1 - \frac{2H_0^2 k^2}{3}\right) \left(1 - \frac{H_0^2 k^2}{3}\right)^{-1/2}, \quad k \leq \frac{\sqrt{3}}{H_0}$	—	$\pm c \left(1 - \frac{H_0^2 k^2}{3}\right)^{1/2}, \quad k \leq \frac{\sqrt{3}}{H_0}$	—	$L_{10}(h, u) = 0, \quad L_{20}(h, u) = -\frac{H_0 c^2}{3} h_{,xxx}$	J. Wisem [1]
C	$\pm \left(1 + \frac{k^2}{3}\right)^{-3/2}$	0	$\pm \left(1 + \frac{k^2}{3}\right)^{-1/2}$	0	$L_{11}(\eta, u) + (u\eta)_x = \frac{1}{3}\eta_{,xx}$ $L_{21}(\eta, u) + uu_x = \frac{1}{3}[L_{21}(\eta, u)]_{,xx}$	J. Bonna and R. Smith [19]
D	$\pm \left(1 + \frac{k^2}{3}\right)^{-3/2}$	0	$\pm \left(1 + \frac{k^2}{3}\right)^{-1/2}$	0	$L_{11}(\eta, u) + (u\eta)_x = 0$ $L_{21}(\eta, u) + uu_x = \frac{1}{3}u_{,xx}$	[19]
E	$\pm \frac{\sqrt{3}}{2} \left[1 + \left(1 + \frac{2}{3k^2}\right)\right] \left[\left(1 + \frac{2}{k^2} \pm \sqrt{1 + \frac{4}{3k^2} + \frac{4}{k^4}}\right)\right]^{-1/2}$ $\times \left(1 + \frac{4}{3k^2 + k^4}\right)^{-1/2}$	$0, \sqrt{3/2}$	$\pm \frac{\sqrt{3}}{2} \left\{ \left(1 + \frac{2}{k^2}\right) \pm \left[\left(1 + \frac{2}{k^2}\right)^2 - \frac{8}{3k^2} \right]^{1/2} \right\}$	0; $\pm \sqrt{3}/\sqrt{2}$	$L_{11}(\eta, u) + (u\eta)_x - \eta\eta_x + \frac{1}{6}\eta_{,xx} = 0$ $L_{21}(\eta, u) + \left(\frac{1}{2}\eta_{,xx} - u\eta\right)_x = 0$	R. Long [17]
F	$\pm c \left(1 + \frac{H_0^2 k^2}{3} + \frac{H_0^4 k^4}{12}\right) \left[\left(\sqrt{1 + \frac{H_0^2 k^2}{6}}\right) \left(1 + \frac{H_0^2 k^2}{2}\right)\right]^{-1}$	$\pm c/\sqrt{3}$	$\pm c \left\{ \left(1 + \frac{H_0^2 k^2}{6}\right) \left(1 + \frac{H_0^2 k^2}{2}\right) \right\}^{-1/2}$	$\pm \frac{c}{\sqrt{3}}$	$L_{10}(h, u) = \frac{1}{6}(H^2 u)_{,xxx}$ $L_{20}(\eta, u) = \frac{1}{2}(H^2 u)_{,xxx}$	C. Mei and B. Le Mehaute [14]
G	$\pm c \left(1 + \frac{H_0^2 k^2}{3} + \frac{H_0^4 k^4}{12}\right) \left[\left(\sqrt{1 + \frac{H_0^2 k^2}{6}}\right) \left(1 + \frac{H_0^2 k^2}{2}\right)\right]^{-1}$	$\pm c/\sqrt{3}$	$\pm c \left\{ \left(1 + \frac{H_0^2 k^2}{6}\right) \left(1 + \frac{H_0^2 k^2}{2}\right) \right\}^{-1/2}$	$\pm \frac{c}{\sqrt{3}}$	$L_{10}(h - B, u) + \frac{1}{2}(H^2 B)_x = \frac{1}{6}(H^2 u)_{,xxx}$ $L_{20}(\eta, u) + (HB)_{,x} = \frac{1}{2}(H^2 u)_{,xxx}$	A Dorfman and G. Yagovdik [16]
H	$\pm c \left(1 + \frac{H_0^2 k^2}{3}\right)^{-3/2}$	0	$\pm c \left(1 + \frac{H_0^2 k^2}{3}\right)^{-1/2}$	0	$L_{10}(h - B, u) + \frac{1}{2}(hh_x)_{,x} = \frac{1}{6}[3(h_x)^2 u + Hh_x u_{,x}]$ $L_{20}(\eta, u) + \frac{1}{2}(hB)_{,x} = \frac{1}{3}(h^2 u_{,xx} + \frac{1}{2}hh_x u_x)$	[16]
K	$\pm c \left(1 + \frac{H_0^2 k^2}{3}\right)^{-3/2}$	0	$\pm c \left(1 + \frac{H_0^2 k^2}{3}\right)^{-1/2}$	0	$L_{10}(h, u) = 0, \quad L_{20}(\eta, u) = \frac{1}{2}H(Hu)_{,xx} - \frac{1}{6}H^2(u_x)_{,x}$	D. Peregrine [11]
L	$\pm c \left(1 - \frac{2H_0^2 k^2}{3}\right) \left(1 - \frac{H_0^2 k^2}{3}\right)^{-1/2}, \quad k \leq \frac{\sqrt{3}}{H_0}$	—	$\pm c \left(1 - \frac{H_0^2 k^2}{3}\right)^{1/2}, \quad k \leq \frac{\sqrt{3}}{H_0}$	—	$L_{10}(h, u) = \frac{1}{2}(H^2(Hu)_{,xx} - \frac{1}{3}H^3 u_{,xxx}), \quad L_{20}(\eta, u) = 0$	[11]

unique, boundaries of phase and group velocities and the ω values connected with this model remain real.

2.2. Finite difference algorithms

Consider problems connected with constructing finite difference approximations of non-linear dispersion models. For simplicity we restrict ourselves to the case of one spatial variable changing in the interval $0 \leq x \leq L$, so that in the inner points of the area a solution satisfies the corresponding system of equations and the boundary conditions at $x = 0$ and $x = L$.

In going to the numerical model, introduce a set of points $X = \{x_0, \dots, x_m; t_0, \dots, t_N\}$ representing the region of changing discrete variables (x_i, t_n) , so that $x_{i+1} - x_i = \Delta x$, $t_{n+1} - t_n = \Delta t$, $f_i^n = f(x_i, t_n)$ and $x_0 = 0$, $x_m = L$. Define discrete operators:

$$\begin{aligned} \mu(f_i) &= \frac{1}{2}(f_{i+1} - f_{i-1}); \quad \Delta_+ f(x) = f(x + \Delta x) - f(x); \\ \Delta_- f(x) &= f(x) - f(x - \Delta x); \quad \Delta f(x) = \Delta_+ \Delta_- f(x); \quad \delta f(x) = (\Delta_+ - \Delta_-)f(x). \end{aligned}$$

Notions of approximation, stability and connected with them definitions, techniques and results are interpreted by us according to monographs [20, 21].

Undertaking to give an account of the main results of the present paragraph, note that publications of recent years, dealing with numerical simulation of wave propagation on the water in the framework of non-linear dispersion models [18, 22], ignore problems of practical realization of boundary conditions, for example, such as "solid wall" and "free boundary". The former describes the wave interaction with the fully reflecting obstacle, and the latter on the contrary, should simulate an "artificial" boundary which allows the approaching wave to pass fully. Realization of physical situations of this kind is necessary when solving problems connected with real problems of propagation and transformation of tsunami waves. Presence of dispersive members, containing spatial derivatives of the second, third and, sometimes, fourth order, requires assigning extra information in constructing finite difference analogs of differential boundary problems. These extra boundary conditions are not conditioned by the mathematical character of the task but exceptionally by the requirements of completeness of the computational algorithm. With it there arises a task to define them in such a way that it should not lead to disastrous consequences for the task as a whole. The aim of our work, in this respect, is to construct some versions of boundary conditions of the above type and to test their efficiency experimentally.

The choice of equations (13)–(14) as a basis for constructing finite difference algorithms is conditioned by the form of equations, permitting the application of various simple difference schemes.

Write system (13) in terms nondimensional variables, introduced by the formulas:

$$(x, y) = \frac{1}{D_0}(x^*, y^*); \quad t = t^* \sqrt{\frac{g}{D_0}}; \quad \eta = \eta^*/D_0; \quad (u, v) = \frac{1}{\sqrt{gD_0}}(u^*, v^*). \quad (25)$$

Such a system will have the following form:

$$\begin{cases} u_t = uu_x + \eta_x = \frac{D}{2} \{(DU)_{xx} - \frac{D}{3} u_{xx}\}_t, \\ \eta_t + [(D + \eta)u]_x = 0 \end{cases} \quad (26)$$

In paper Ref. [11] for the system of equations (26) there was suggested an implicit two-level

finite difference scheme with recalculation:

$$\begin{aligned}
 & \frac{u_i^{\eta+1} - u_i^\eta}{\Delta t} + \frac{u_i^\eta}{2\Delta x} \delta \left(\frac{u_i^{\eta+1} + u_i^\eta}{2} \right) + \frac{1}{2\Delta x} \delta \left(\frac{\eta_i^* + \eta_i^\eta}{2} \right) \\
 &= \frac{1}{(\Delta x)^2} \frac{D_i^2}{3} \Lambda \left(\frac{u_i^{\eta+1} - u_i^\eta}{\Delta t} \right) + \frac{D_i}{2(\Delta x)^2} \Lambda(D_i) \frac{u_i^{\eta+1} - u_i^\eta}{\Delta t} \\
 &+ \frac{D_i}{2\Delta x} \delta \left\{ \frac{D_i}{2\Delta x} \right\} \delta \left(\frac{u_i^{\eta+1} - u_i^\eta}{\Delta t} \right), \\
 &\times \frac{\eta_i^* - \eta_i^\eta}{\Delta t} + \frac{1}{2\Delta x} (D_i + \eta_i^\eta) \delta(u_i^\eta) + \frac{u_i^\eta}{2\Delta x} \delta(D_i + \eta_i^\eta) = 0, \\
 &\frac{\eta_i^{\eta+1} - \eta_i^\eta}{\Delta t} + \frac{(D_i + \eta_i^\eta)}{2\Delta x} \delta \left(\frac{u_i^{\eta+1} + u_i^\eta}{2} \right) + \frac{u_i^{\eta+1} + u_i^\eta}{4\Delta x} \delta(D_i + \eta_i^\eta) = 0, \tag{27}
 \end{aligned}$$

having the first order of approximation in time and the second one on spatial variables. Spectral analysis of the linearized version of scheme (27) and numerical experiments enable one to understand the unconditional stability of the algorithm.

We shall show, that by studying the second differential approximation [23] of equation (27) one can get some additional information about the approximation of the process of long wave propagation by this scheme. Note that in the deriving system (26) the method of function expansion into a power series of the small parameter ϵ and retention of members accurate up to the second order of size was used. This means, that the sought values can be presented in the form [11]:

$$\mathbf{u} = \epsilon \mathbf{u}_1 + \epsilon^2 \mathbf{u}_2, \quad \eta = \epsilon \eta_1 + \epsilon^2 \eta_2, \tag{28}$$

in assuming that $\mathbf{u}_0 = \eta_0 = 0$. Herein it was assumed that nondimensional variables were scaled so that:

$$\frac{\partial}{\partial x} = \sigma \frac{\partial}{\partial x_1}, \quad \frac{\partial}{\partial y} = \sigma \frac{\partial}{\partial y_1}, \quad \frac{\partial}{\partial t} = \sigma \frac{\partial}{\partial t_1}. \tag{29}$$

The variables η_i , \mathbf{u}_i , $D(x_i)$ and their x_1 , y_1 , t_1 derivatives are assumed to be quantities of $O(1)$ order. It is also assumed that $\epsilon \sim \sigma^2$.

Now using equations (28) and (29) one can estimate the value of each member of equation (26):

$$\begin{aligned}
 \eta_i \sim \eta_x \sim u_i \sim O(\sigma^3) + O(\sigma^5), \quad [(D + \eta)u]_x \sim uu_x \sim O(\sigma^5) + O(\sigma^7) + O(\sigma^9), \\
 D^2 u_{ixx} \sim D(Du)_{ixx} \sim O(\sigma^5) + O(\sigma^7).
 \end{aligned}$$

Write out the second differential approximation of scheme (27):

$$\begin{aligned}
 & u_i + uu_x + \eta_x + \frac{\Delta t}{2} \{u_{ii} + uu_{ix} - [(D + \eta)u_{xx}]\} + \frac{(\Delta t)^2}{4} u_{iix} + \frac{(\Delta t)^2}{6} u_{iii} + \frac{(\Delta x)^2}{6} (\eta_{xxx} + uu_{xxx}) \\
 &= \frac{D}{2} (Du)_{ixx} - \frac{D^2}{6} u_{ixx} + \frac{\Delta t}{2} \left(\frac{D^2}{3} u_{iixx} + DD_x u_{iix} + \frac{D}{2} D_{xx} u_{ii} \right) \\
 &+ \frac{(\Delta t)^2}{6} \left\{ \frac{D^2}{3} u_{iixx} + DD_x u_{iix} + \frac{D}{2} D_{xx} u_{iii} \right\} \\
 &+ \frac{(\Delta x)^2}{6} \left(\frac{D^2}{6} u_{iixx} + DD_x u_{iixx} + DD_{xxx} u_{ix} + \frac{D}{4} D_{xxxx} u_i \right), \\
 &\eta_i + [(D + \eta)u]_x + \frac{\Delta t}{2} \{ \eta_{ii} + (D + \eta) u_{ix} + (D + \eta)_x u_i \} \\
 &+ \Delta t^2 \left\{ \frac{1}{6} \eta_{iii} + \frac{(D + \eta)}{4} u_{iix} + \frac{1}{4} (D + \eta)_x u_{ii} \right\} + \frac{(\Delta x)^2}{6} \{ (D + \eta) u_{xxx} + u(D + \eta)_{xxx} \} = 0. \tag{30}
 \end{aligned}$$

Subject to the system of equation (26), dropping members of greater order of infinitesimal than $O(\epsilon^3)$, from equation (30) one can get the system:

$$\begin{aligned}
 u_t + uu_x + \eta_x - \frac{\Delta t}{2} u_t u_x + \frac{(\Delta t)^2}{6} u_{ttt} + \frac{(\Delta x)^2}{6} \eta_{xxx} + \frac{(\Delta t)^2}{4} u_{ttx} &= \frac{D}{2} (Du)_{txx} - \frac{D^2}{6} u_{txx}, \\
 \eta_t + [(D + \eta)u]_x - \frac{\Delta t}{2} (\eta_{tx} u + \eta_t u_x) + \Delta t^2 \left(\frac{\eta_{ttt}}{6} + \frac{D}{4} u_{ttx} + \frac{D_x u_{tt}}{4} \right) + \frac{(\Delta x)^2}{4} (Du_{xxx} + uD_{xxx}) &= 0.
 \end{aligned}
 \tag{31}$$

So that system (31) should conserve hydrodynamical approximation properties intrinsic of the initial system (26). It is necessary for the members, introduced at the finite difference approximation, to have the order of infinitesimal not lower than $O(\sigma^3)$, for which the relations

$$\Delta t \sim O(\sigma^3), \quad \Delta t / \Delta x \sim O(\sigma).
 \tag{32}$$

must be satisfied.

For the approximation of system (26) we have also suggested a three-level scheme:

$$\begin{aligned}
 \frac{u_i^{\eta+1} - u_i^{\eta-1}}{2\Delta t} + \frac{u_i^\eta}{2\Delta x} \delta u_i^\eta + \frac{\delta \eta_i^\eta}{2\Delta x} &= \frac{D_i}{3(\Delta x)^2} A \left(\frac{u_i^{\eta+1} - u_i^{\eta-1}}{2\Delta t} \right) \\
 + \frac{D}{2\Delta x} \delta \left(\frac{D}{2\Delta x} \right) \delta \left(\frac{u_i^{\eta+1} - u_i^{\eta-1}}{2\Delta t} \right) + \frac{D_i}{2(\Delta x)^2} (AD_i) &\left(\frac{u_i^{\eta+1} - u_i^{\eta-1}}{2\Delta t} \right), \\
 \frac{\eta_i^{\eta+1} - \eta_i^{\eta-1}}{2\Delta t} + \frac{(D_i + \eta_i^\eta)}{2\Delta x} \delta u_i^\eta + \frac{u_i^\eta}{2\Delta x} \delta (D_i + \eta_i^\eta) &= 0.
 \end{aligned}
 \tag{33}$$

Equation (33) has the second order of approximation in time and space. The study of the hydrodynamical approximation properties leads to the consideration of the analog of equations (31) having the form:

$$\begin{aligned}
 u_t + uu_x + \eta_x + \frac{(\Delta t)^2}{6} u_{ttt} + \frac{(\Delta x)^2}{6} \eta_{xxx} &= \frac{D}{2} (Du)_{txx} - \frac{D^2}{6} u_{txx}, \\
 \eta_t + [(D + \eta)u]_x + \frac{(\Delta t)^2}{6} \eta_{ttt} + \frac{(\Delta x)^2}{6} (Du_{xxx} + uD_{xxx}) &= 0.
 \end{aligned}
 \tag{34}$$

An analysis of equations (34) shows that it conserves the order of hydrodynamical approximation intrinsic to system (26) under the condition:

$$\Delta t \sim \Delta x = O(\sigma).
 \tag{35}$$

The investigation of stability of equations (33), carried out with a linear analog of equations (26) for the basin with constant depth:

$$\begin{cases} u_t + Uu_x + \eta_x = \frac{D_0}{3} u_{txx}, \\ \eta_t + \Phi u_x + U\eta_x = 0 \end{cases}$$

where U, Φ, D_0 are constants, results in limiting for Δt of the form:

$$\Delta t \leq k \Delta x, \quad \text{where } k = O(\sigma).
 \tag{36}$$

Comparing equations (32), (35) and (36) if equations (27) and (33) are required to be the same order of hydrodynamical approximation in terms of the order of infinitesimal of the members, retained in equations (31) and (33) respectively, then unconditional stability of scheme (27) does not give advantage in the size of time step over equations (33). In numerical experiments schemes (27) and (33) behave steadily at:

$$\Delta t \leq \Delta x / \sqrt{gD_0}.$$

Further we dwell upon a brief description of two difference schemes for system (14) in its 1-D version. The first one, having the order of approximation $O(\Delta t, \Delta x^2)$, is given by the authors of Ref. [12]:

$$\begin{aligned} \frac{u_i^{\eta+1} - u_i^\eta}{\Delta t} + \frac{u_i^\eta}{2\Delta x} \delta u_i^\eta + \frac{g}{2\Delta x} \delta \eta_i^\eta &= 0, \\ \frac{\eta_i^{\eta+1} - \eta_i^\eta}{\Delta t} + \frac{1}{2\Delta x} \delta \{(D_i + \eta_i^\eta) u_i^{\eta+1}\} &= - \left\{ \frac{D_i^2}{4\Delta x^3} \Lambda(\delta u_i^{\eta+1}) + \frac{D_i}{2\Delta x} \delta(D_i) \frac{1}{\Delta x^2} \Lambda(D_i u_i^{\eta+1}) \right. \\ &\quad \left. - \frac{D_i^3}{12\Delta x^3} \Lambda(\delta u_i^{\eta+1}) - \frac{D_i}{4\Delta x} \delta(D_i) \frac{1}{\Delta x^2} \Lambda(u_i^{\eta+1}) \right\}. \end{aligned} \quad (37)$$

Spectral analysis of stability of its linear analog results in the condition:

$$\Delta t \leq \Delta x / \sqrt{gD_0} \quad (38)$$

however, numerical experiments require to enhance this condition:

$$\Delta t \leq 0.1 \Delta x / \sqrt{gD_0}. \quad (39)$$

One can attempt to improve stability properties at the expense of introducing smoothing procedures. Consider from this view-point the following scheme:

$$\begin{aligned} \frac{u_i^{\eta+1} - [k_u u_i^\eta + (1 - k_u) \mu(u_i^\eta)]}{\Delta t} + \frac{u_i^\eta}{2\Delta x} \delta(u_i^\eta) + \frac{g}{\Delta x} \Delta_-(\eta_i^\eta) &= 0, \\ \frac{\eta_i^{\eta+1} - [k_\eta \eta_i^\eta + (1 - k_\eta) \mu(\eta_i^\eta)]}{\Delta t} + \frac{1}{\Delta x} \Delta_+ [\mu(\eta_i^\eta + D_i) u_i^{\eta+1}] \\ &= \frac{D_i^2}{2\Delta x} \Delta_+ \left(\frac{1}{\Delta x^2} \Lambda(D_i u_i^{\eta+1}) \right) + \frac{D_i}{\Delta x} \Delta_+(D_i) \left\{ \frac{1}{\Delta x} \Delta_+ \left[\frac{\delta(D_i u_i^{\eta+1})}{2\Delta x} \right] \right\} \\ &\quad - \frac{D_i^3}{8\Delta x} \Delta_+ \left(\frac{1}{\Delta x^2} \Lambda u_i^{\eta+1} \right) - \frac{D_i^2}{2\Delta x} \Delta_+(D_i) \frac{1}{\Delta x} \Delta_+ \left[\frac{1}{2\Delta x} \delta(u_i^{\eta+1}) \right]. \end{aligned} \quad (40)$$

In equations (40) the parameters k_u and k_η determine the value of artificial viscosity reaching maximum at $k_u = k_\eta = 0$. A numerical experiment showed that the optimal choice of these parameters is $k_u = 0, k_\eta = 1/2$. At other values the scheme either loses stability or artificial viscosity appears abundant and the profile of a simulated wave "smears" quickly. Equations (40) has the order of approximation $O(\Delta t, \Delta x^2)$ at $k_u = k_\eta = 1$ and $O(\Delta t, \Delta x)$ in other cases. The stability condition of a linear analog of equations (40) is as follows:

$$1 > k > 1 - gD_0 \left(\frac{\Delta t}{\Delta x} \right)^2 > 0, \quad \text{where } k = \text{mod}(k_u, k_\eta).$$

Note that the above equations (27), (33) and (37) are constructed so that both the unknown functions are defined in one mesh point of the calculated region. However, from the view-point of a numerical realization of boundary conditions, it is more convenient to construct a difference scheme so that one of the quantities, for example velocity, should be determined at mesh points with the coordinates $i\Delta x$, and the quantity of the wave height determined at mesh points with the coordinates $(i + \frac{1}{2})\Delta x$. This approach has been realized on constructing equations (40). Also note, that the last equations (37) and (40) belong to the class of explicit-implicit difference schemes, since in the second differential equation the already numbered qualities of one of the unknown functions are used.

Striving to obtain a maximum economical algorithm leads to an attempt to work out some criteria permitting the division of the calculated region into subregions, in the part of which dispersion effects are considered negligible and counting is made by equations of the shallow water theory. The simplest criteria of this kind is some threshold value of the basin depth. Dispersion in the deep-water part is not taken into account. Such a match of two models, as well as the influence of boundaries, deteriorates numerical stability and

requires the introduction of extra smoothing operators, functioning in adhesive joints. The approximation of the third derivatives results in generating parasitic high-frequency harmonics.

Proceed to the description of realizing boundary conditions. Firstly, consider the situation, when in the boundary points $x_0 = 0$, $x_m = L$ an assumption is made of the existence of fully reflecting obstacles. This means that velocity in the direction of the normal to the "wall" equals zero. Since information about points neighboring the boundary is necessary for a numerical simulation with the above described schemes, one has to use extra mesh points. Also it is assumed that "the wall" was in the node with the number i_0 , the corresponding boundary conditions in the terms of velocity can be presented by the relations:

$$u_{i_0} = 0, \quad u_{i_0+1} = -u_{i_0-1}, \quad u_{i_0+2} = -u_{i_0-2}. \quad (41)$$

The account of dispersion at the near-boundary points requires formulation of the boundary conditions for the function η which can be naturally presented in the form:

$$\frac{\partial \eta}{\partial n} = 0, \quad x = 0, \quad x = L; \quad (42)$$

or

$$\eta_{i_0+1} = \eta_{i_0-1}, \quad \eta_{i_0+2} = \eta_{i_0-2}.$$

One may also suggest the calculation in the near-boundary region, by the linear equations of the shallow water theory [equation (9)] to determine the quantities u , η in different nodes. In this case to describe a boundary condition "wall" it is sufficient to have either equations (41) or (42).

In Figure 1 the results of a numerical testing of boundary conditions equations (41) and (42) are shown. The calculation was made by equations (37) for a basin with constant depth. The initial state of the basin surface was determined by the relation:

$$\eta(x, 0) = \eta_0 \operatorname{sech}^2 \left[\left(\frac{3\eta_0}{4D^3} \right)^{1/2} (x - x_0) \right], \quad (43)$$

and velocity at the initial moment equalled zero. With it the initial impulse fell into two waves, each having the amplitude $\eta_0/2$, propagating in opposite directions. Reaching the boundaries of the basin, these waves are reflected and go towards each other. Some deformation of the wave form, observed here, is due to dispersion properties of the model (the value of Ursell's parameter $U \sim 1.25$). Also note that the reflection of solitary waves, equation (43), from the boundary is equivalent to the collision of two such waves of the same amplitude.

The necessity of a boundary condition, describing the outlet of disturbance beyond the boundaries of the calculated region, arises on solving tasks in essentially bounded regions of changing spatial variables when at the boundary of the region it is impossible to formulate some *a priori* physical conditions—periodicity, symmetry etc. The most acceptable, in terms of the magnitude of introduced errors and simplicity of realization, is a boundary condition, expressing the assumption of the transfer of disturbance over the boundary without changing its form, with the velocity equal to the propagation velocity of this disturbance near the boundary. This boundary condition coincides with the first approximation to the absolutely absorbing boundary condition [24].

Thus, it is assumed, that in the near-boundary points the wave behavior is described by the transfer equation:

$$\frac{\partial \eta}{\partial t} + c \frac{\partial \eta}{\partial n} = 0, \quad (44)$$

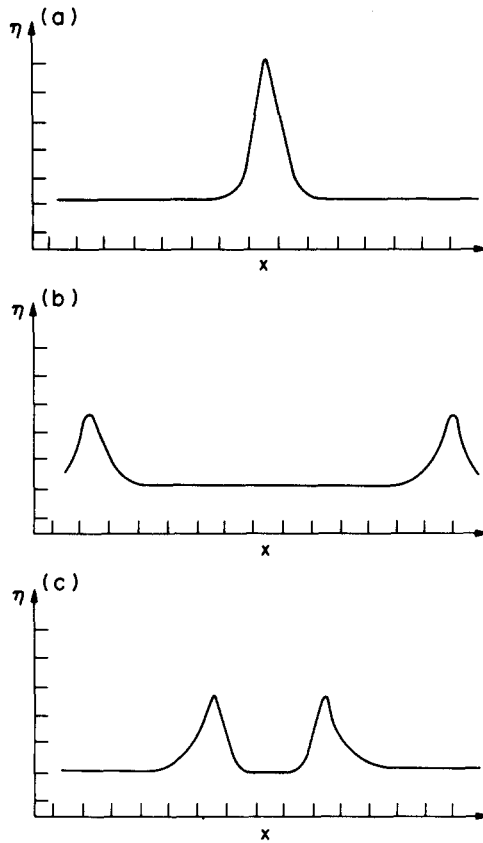


Fig. 1. Interaction of a solitary wave with fully reflecting boundaries. Equations (37), boundary condition equations (41) and (42); (a) initial profile; (b) waves at the reflecting boundaries; (c) waves after reflection.

where $\partial/\partial n$ is a derivative in the direction of the external normal to the boundary under consideration. Discretization of equation (44) leads to the relation:

$$\eta_{rp}^{\eta+1} = \eta_{rp}^{\eta} + \frac{c \Delta t}{\Delta n} (\eta_{rp}^{\eta} - \eta_{nrp}^{\eta}), \tag{45}$$

where η_{rp}, η_{nrp} are the values of the wave height in the boundary and in the nearest to the boundary points, in the direction n . Formula (45) is an interpolation one whose stability is provided by satisfying the condition:

$$c \Delta t / \Delta x \leq 1.$$

A numerical solution of equations with dispersive members requires, as mentioned above, setting extra boundary relations for the velocity near the absorbing boundary. This can be done for example:

$$u_r = c\eta / (D + \eta), \quad c = \sqrt{gD} \tag{46}$$

However, in the framework of non-linear dispersion models, the wave propagation velocity is described by the formula $c = \sqrt{gD}$ inaccurately, which allows one to somewhat improve the boundary condition, determining in equation (46) the quantity c by the relation:

$$c = [(D + \eta)u]_x / \eta_x,$$

which is the consequence of equation (44). This allows a boundary condition to be constructed in the form:

$$\frac{\partial u}{\partial t} + \tilde{c} \frac{\partial u}{\partial n} = 0, \tag{47}$$

where

$$\tilde{c} = \begin{cases} [(Dc + \eta)u]_x / \eta_x & \text{at } |\eta_x| \geq \epsilon_0 \\ \sqrt{gD} & \text{at } |\eta_x| < \epsilon_0 \end{cases} \quad (48)$$

The quantities of derivatives in equation (48) are calculated in the near-boundary points.

In Figure 2 are depicted the results of calculations of the version analogous to that described previously with the only difference that approaching the boundaries, which now simulate the condition of a free passage, the waves go beyond the boundaries of the region, reflecting inside a wave, whose maximum amplitude does not exceed 8% of the amplitude of the initial impulse. The mareogram calculated in the near-boundary point (i.e. the function representing the change of level of the liquid surface with time at this point), demonstrates practically a complete preservation of the wave form on its going out beyond the region. The results, presented in Fig. 2, have been obtained by the equations (37) using boundary conditions in equations (45) and (46). The boundary condition in equations (45), (47) and (48) was tested in combination with the schemes (27) and (33). In Figures 3 (a) and (b) the profiles of free surface are calculated for different moments of time by equations (33) with the boundary conditions in equations (45), (46) and (45), (47), (48), respectively. The use of the boundary condition in equations (45) and (46) result in the growth of amplitude of a going away wave by 1.8%, some increase of its length and the appearance of a reflected wave with the amplitude of 2.3% of the initial impulse amplitude. When substituting the boundary condition with equations (45), (47) and (48) practically no increase of the wave length occurs. Its amplitude changes by 0.6% and the amplitude of a reflected wave decreases more than two times. The noted advantages of the boundary

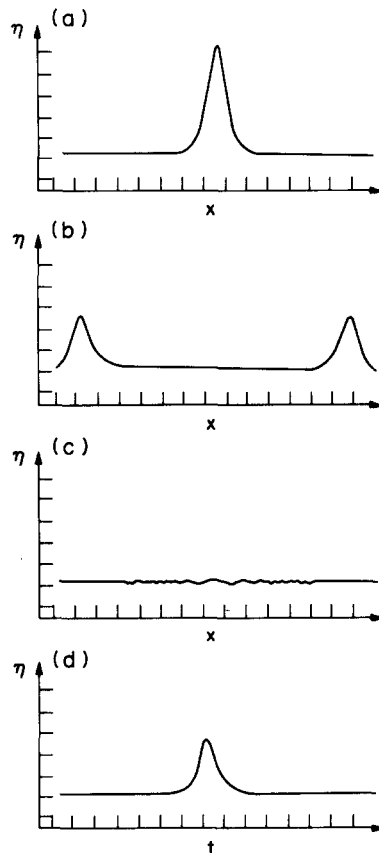


Fig. 2. The interaction of a solitary wave with a "free" boundary. Equations (37), boundary condition equations (45) and (46); (a) the initial profile; (b) waves at the free boundaries; (c) the basin surface after the wave passing; and (d) the mareogram calculated at the "free" boundary.

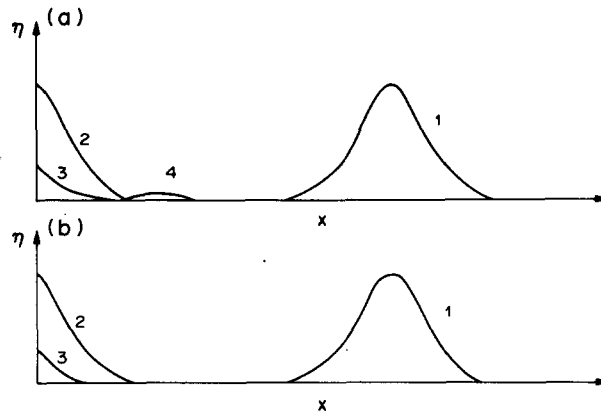


Fig. 3. The interaction of a solitary wave with a "free" boundary. Equations (33); (a) the boundary condition equations (45) and (46); (b) the boundary condition equations (45), (47) and (48).

condition in equations (45), (47) and (48) are exhibited in a more contrasting way on counting by the equations (27) [see Fig. 4(a)—the boundary condition in equations (45) and (46), and Fig. 4(b)—the boundary condition in equations (45), (47) and (48)]. In this case the first boundary condition results in an increase in the amplitude of an outgoing wave by 2.7% (0.2% for the second boundary condition) and the appearance of a reflected wave with the amplitude 2.3% of the initial impulse amplitude (a corresponding quantity for the second boundary condition is 0.7%).

3. NUMERICAL SIMULATION OF LONG WAVES PROPAGATION IN SHALLOW WATER IN THE FRAMES OF APPROXIMATED NON-LINEAR HYDRODYNAMICAL MODELS

The next series of calculations was undertaken to elucidate questions of influence of non-linear and dispersion effects on the wave propagating in the shallow zone depending on its initial characteristics and parameters of the bottom relief. This range of questions is connected with the problems of the paper Ref. [18], whose results allow one to conclude that the influence of these effects becomes considerable at the depths < 80 m. At the same time a numerical technique, developed and applied in Ref. [18], proves unstable at depths from 45 m and less for gently sloping shelves (with the slope $\alpha \approx 0.5^\circ$) and at the depths from 69 m and less for steep shelves (with the slope $\alpha \approx 1^\circ$). Thus, one can say that our calculations cover the most interesting part of the process occurring in the basin, whose depth decreases from 20 to 2 m.

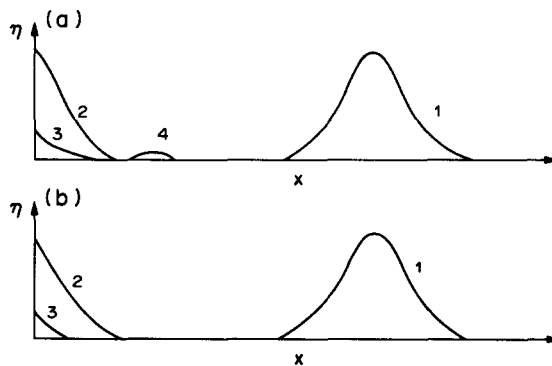


Fig. 4. The interaction of a solitary wave with a "free" boundary. Equations (27); (a) the boundary condition equations (45) and (46); (b) the boundary condition equations (45), (47) and (48).

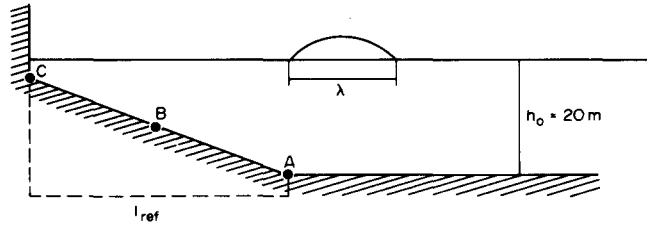


Fig. 5. The scheme of a model basin.

Consider a model basin schematically depicted in Fig. 5. Its maximum depth $D_0 = 20$ m, and minimum $D_M = 2$ m. Points A, B, C are situated at the beginning, at the middle and at the end of the slope, respectively. We shall assume that the boundary condition at the point $x_0 = 0 [D(x_0) = D_M]$ describes a full reflection of the wave from the shore and at the “marine” boundary $x_M = L [D(x_M) = D_0]$ a condition of the free passage is set. At the initial moment of time the water surface has the form of a solitary wave, whose maximal amplitude is reached at the point x_* , $[D(x_*) = D_0]$. Setting a corresponding field of velocities:

$$u(x, 0) = -(1 + \eta_0/2)\eta(x, 0)/[D + \eta(x, 0)], \tag{49}$$

provides a directed wave propagation from the region of the constant depth D_0 to the shore. Results obtained on the account of non-linear dispersion effects are denoted by the symbol (ND); results obtained only taking into account convective non-linearity are denoted by the symbol (N) and, finally, data calculated by equation (2) are denoted by the symbol (L). We shall also name the distance between points, in which the wave height is equal to $0.01 \eta_0$, by the wave length λ .

The mareograms, shown in Fig. 6, calculated in the middle of the slope (ND) for waves with different lengths of initial perturbation, obviously demonstrate the strengthening of dispersion effects with decreasing λ . (Ursell’s parameter decreases with it from 40 to 2.5.) The steepness of the front slope also increases. Note that the dispersion effects determine the behaviour of both falling and reflected waves.

Considering the mareograms, numbered at the beginning of the slope by three mathematical models (see Fig. 7), we see, that for waves with the parameters $\lambda = 400$ m, $U = 40$, the influence of non-linear and dispersion effects is negligible in comparison with the short wave ($\lambda = 100$ m, $U = 2.5$), whose mareogram represents a record of the falling wave and a strongly dispersive sequence of reflected waves immediately joining it.

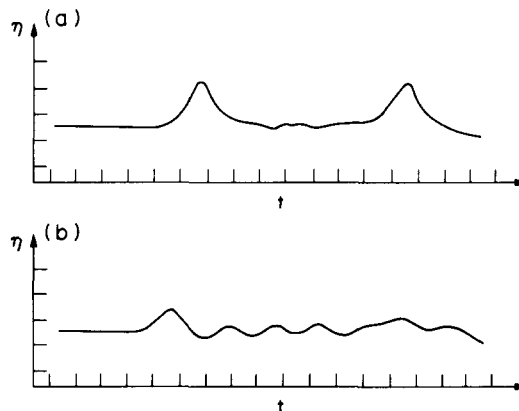


Fig. 6. Influence of the initial impulse length on characteristics of the mareograms calculated at the point B (the middle of the slope). Model (ND). $\eta = 2$ m, $L_{ref} = 500$ m; (a) $\lambda = 400$ m, (b) $\lambda = 100$ m.

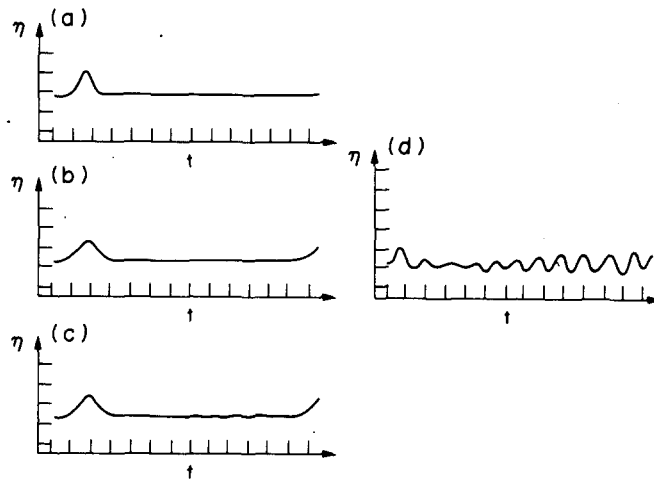


Fig. 7. Influence of non-linear and dispersion effects on characteristics of the mareograms calculated at the point A (the foot of the slope). $\eta_0 = 2$ m, $L_{ref} = 500$ m; (a) model (L), $\lambda = 400$ m; (b) model (N), $\lambda = 400$ m; (c) model (ND), $\lambda = 400$ m; (d) model (ND), $\lambda = 100$ m.

At the vertex of the slope, i.e. on the shore, the wave behaviour is determined mainly by convective, non-linear effects, which is convincingly testified by the results, presented in Fig. 8. As seen, the mareograms (N) and (ND) are practically indistinguishable while the (L) wave practically manages to be fully reflected during the passing time of the slope. This effect is traced in detail in Fig. 9, where two series of wave profiles are depicted, calculated for different time moments by the models (L) and (N). As seen in the figure the (L) wave is practically fully reflected before the middle of the slope, while the (N) wave, increasing its steepness, rises up to the vertex of the slope, is reflected and goes into a relatively deep-water part.

Increasing amplitude of the initial impulse, we have the right to rely upon a proportional change of results, calculated by equation (9). Yet here too we are faced with an unexpected counting effect bridging a non-linearity effect. Thus in Figure 10 the wave profiles and mareograms are depicted, calculated by the linear model equation (9) for the initial impulse with the amplitude $\eta_0 = 10$ m. At that a substantial part of the wave with the amplitude about 5.7 m overcomes the reflection of the sloping bottom and reaches the vertex of the slope. The height of the wave at the vertex exceeds that of the wave approaching the beginning of the slope by 1.3 times, and the period of the wave increases by 1.5 times. The

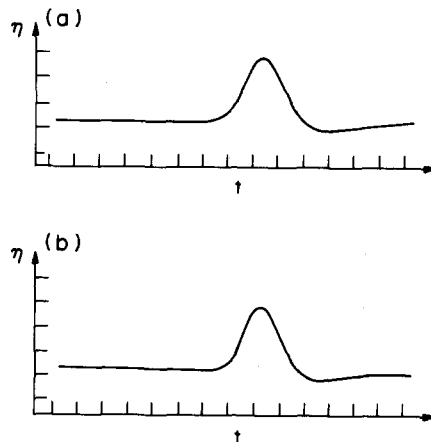


Fig. 8. The mareograms calculated at the point C (the vertex of the slope). $\eta_0 = 2$ m, $L_{ref} = 500$ m, $\lambda = 400$ m, (a) model (N), (b) model (ND).

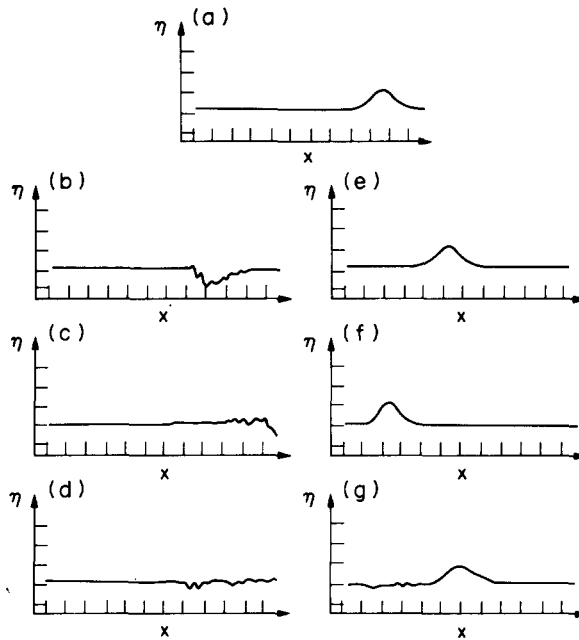


Fig. 9. The profiles of a free surface of the model basin at different time moments: (a) $T = 0$; (b) model (L) and (e) model (N) at $T = 15$; (c) model (L) and (f) model (N) at $T = 30$; (d) model (L) and (g) model (N) at $T = 60$. $\eta_0 = 2$ m, $L_{ref} = 500$ m, $\lambda = 400$ m.

same increase of the initial impulse amplitude intensifies a dispersive character of behaviour of the reflected (ND) wave and results in increasing amplitudes of (N) and (ND) waves having moved against the reflection of the slope (see Fig. 11).

Now we consider the influence of such a factor as the length of the slope. An analysis shows (see Fig. 12), that the decrease of the slope length leads to the effect analogous to

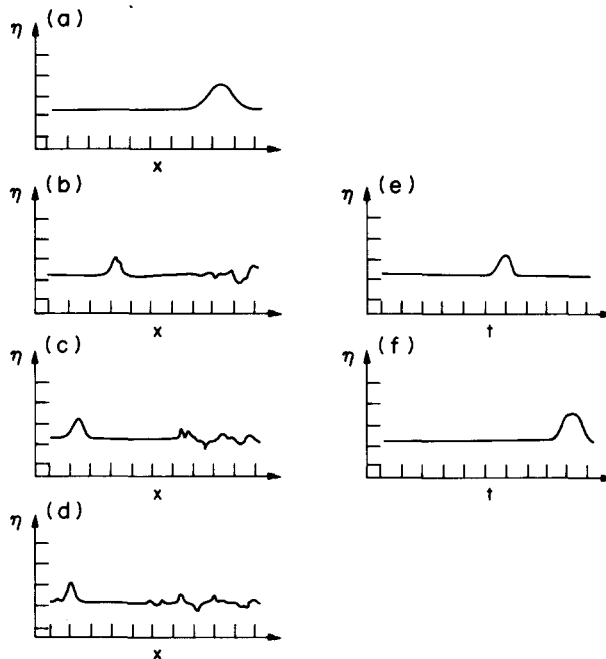


Fig. 10. The change of wave characteristics with increasing the initial impulse amplitude up to 10 m. Model (L) the profiles of a free surface at different time moments: (a) $T = 0$, (b) $T = 40$, (c) $T = 60$, (d) $T = 80$. The mareograms: (e) at the point A (the foot of the slope); (f) at the point C (the vertex of the slope); $L_{ref} = 500$ m, $\lambda = 400$ m.

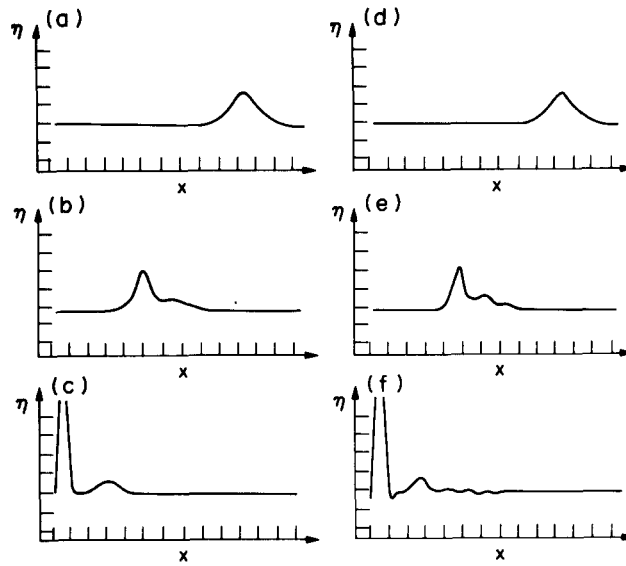


Fig. 11. The change of wave characteristics with increasing the initial impulse amplitude up to 10 m. The profiles of a free surface at different time moments: (a) model (N) and (d) model (ND) at $T = 0$; (b) model (N) and (e) model (ND) at $T = 40$; (c) model (N) and (f) model (ND) at $T = 60$. $L_{ref} = 500$ m, $\lambda = 400$ m.

the decrease of the length of the wave approaching this slope. It is seen on the (ND) mareograms calculated at the beginning of the slope, that both for a short wave on the long gentle slope ($\lambda = 100$ m, $L_{ref} = 1000$ m) and for a long wave on the steep slope ($\lambda = 400$ m, $L_{ref} = 100$ m), the reflected wave immediately follows the approached impulse and represents an intensively dispersing wave train.

The expounded results allow us to draw some qualitative conclusions. Specifically, the mareograms calculated at the points *A*, *B*, *C* allow one to analyse in detail characteristics of both initial and reflected waves and also the dynamics of their change as they move off from the beginning of the slope. Thus, the wave length decreases, when propagating up the slope, the propagation velocity fall leads to a substantial increase of a wave period observed at the vertex of the slope in comparison with the period of the wave approaching the beginning of the rise. Such quantitative characteristics as the ration of the wave amplitude at the vertex to the wave amplitude at the foot of the slope are in a good agreement with results obtained in Ref. [18] by another non-linear dispersion model by the method of characteristics.

Extremely important from the view-point of the choice of a mathematical model for the solution of tasks of a real tsunamizing is a conclusion on the permissibility of applying

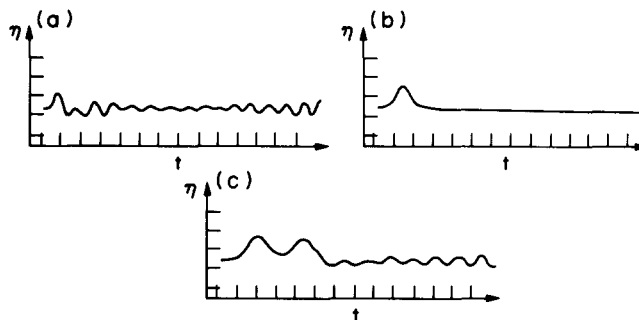


Fig. 12. The change of wave characteristics depending on the extent of rise and the length of the initial impulse. The mareograms calculated at the point A (the foot of the slope). $\eta_0 = 2$ m; (a) $L_{ref} = 1000$ m, $\lambda = 100$ m; (b) $L_{ref} = 1000$ m, $\lambda = 400$ m; (c) $L_{ref} = 100$ m, $\lambda = 400$ m.

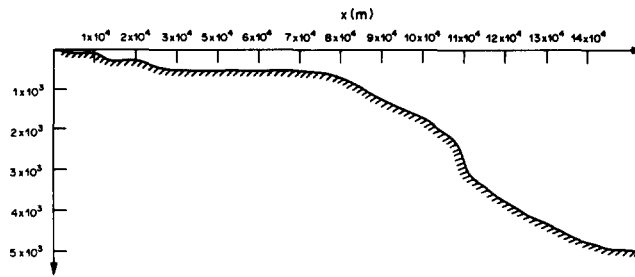


Fig. 13. Distribution of depths along the real wave tube.

a simple and economical linear model, equation (9), for the calculation of sufficiently long wave propagation up to the depths of 20 m. The formulation of a fully reflecting boundary condition at such a depth proves natural.

The results of the first two points of the present paragraph allow us to speak about a finite-difference modelling of non-linear dispersion effects of a long wave propagation in the shoal, which are characteristic of physical processes.

To conclude, we discuss the computation results of tsunami wave propagation along the wave tube with a real relief of the bottom. The homogeneity of the width of this tube along all its length allows one to consider a process in the framework of 1-D equations (26). The bottom relief (see Fig. 13) is so that its maximum depth is 4950 m, its minimum one is 10 m, at a considerable extent the depth does not exceed 1000 m. As initial data an elevation of the water surface is set in the form of a positive semi-sinusoid of 90 km long and the maximum amplitude $\eta_0 = 2$ m attained at the distance of 184 km from the coastline. The perturbation is assumed to be static so that the velocity at the initial moment is equal to zero. Such initial conditions correspond to the instant elevation of the ocean surface as a result of an earthquake at the foot of a continental slope.

The calculation was made from equations (27) for the boundary conditions, from equations (45) and (48) for a "marine" boundary and from equations (41) and (42) for near the shore. The parameters of a difference scheme $\Delta t = 4$ s, $\Delta x = 1000$ m were chosen from the experimental stability condition:

$$\Delta t \leq \Delta x / \sqrt{gD_{\max}}$$

In Figure 14(a) a mareogram is presented calculated at a 10 m isobath. Its analysis shows that a tsunami wave reaches the shore in 29 min and a maximum height of the wave is 6.5 m. The obtained results were compared with the results [see Fig. 14(b)] of the

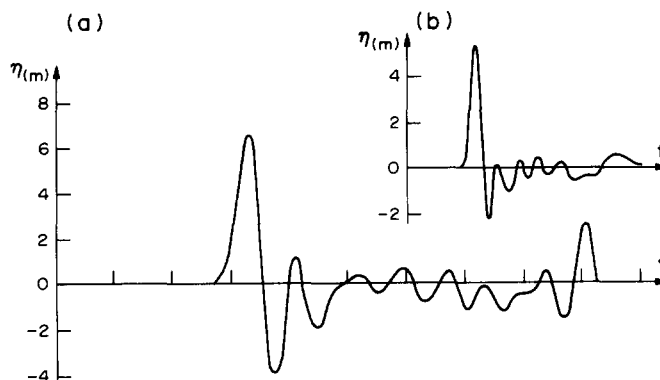


Fig. 14. The mareograms calculated at 10 m depth near the coast. (a) subject to non-linear and dispersion effects; (b) not subject to dispersion effects.

calculation by non-linear equations of the shallow water theory subject to the bottom friction in the form:

$$\alpha u |u| / (D + \eta), \quad (\alpha = 0.26 \times 10^{-2}), \quad (50)$$

added to the movement equation (V. G. Bukhteyev and A. V. Nekrasov).

A refusal from the account of dispersion effects slightly changes the form of oscillations. A wave height decreases by 15% and is 5.5 m, and the time of a wave run from the source to the shore reduces to 25 min (i.e. by 13%).

To appreciate the contribution of the bottom friction, a dissipative member of equation (50) was included in the right side of the movement equation of the system (26). As a result the maximum wave height decreased by 4 sm (0.6%) so that the account of dispersion effects proves more essential than that of the bottom friction.

REFERENCES

1. J. Wizem, *Lineinye i Nelineinye Volny*, p. 622, Mir, Moscow (1977).
2. L. N. Sretensky, *Teoria Volnovykh Dvizheny*, p. 815, Nauka, Moscow (1977).
3. J. Boussinesq, Théorie de l'intumescence liquide appelée onde solitaire on de translation se propageant dans un canal rectangulaire. *Comptes Rendus* **72**, 755 (1871).
4. M. A. Lavrentiev, Do teorii dovgikh hvil. *Zb. Prats Inst. Matem.* **8**, 13 (1946).
5. D. J. Korteweg and G. de Vries, On the change of form of long waves advancing in a rectangular channel, and on a new type of long stationary waves. *Phil. Mag.* **5**, 422 (1895).
6. L. A. Ostrovsky and Ye. N. Pelinovsky, *Nelineinaya evolutsia voln tipa tsunami*. V sb.: *Teoreticheskie i Experimentalnye Issledovaniya po Probleme Tsunami*. p. 52, Nauka, Moscow (1977).
7. K. O. Friedrichs, On the derivation of the shallow water theory. Appendix to the formulation of breakers and bores by J. J. Stoker. *Commun. Pure appl. Math.* **1**, 109 (1948).
8. J. B. Keller, The solitary wave and periodic waves in shallow water. *Commun. Pure appl. Math.* **1**, 323 (1948).
9. J. J. Stoker, *Water Waves*, p. 617, Interscience, New York (1957).
10. L. V. Ovsiannikov, *K obosnovaniu teorii melkoi vody*. V sb.: *Dinamika Sploshnoi Sredy*, Vol. 15, p. 104. Novosibirsk, (1973).
11. D. H. Peregrine, Long waves on a beach. *J. Fluid Mech.* **27**, 815 (1967).
12. M. Chen, D. Divoky and L.-S. Hwang, *Nearfield Tsunami Behaviour.—Final Report*, p. 68, Tetra Tech Inc., Pasadena (1975).
13. V. F. Ivanov and L. V. Cherkosov, Ob uravneniakh Kortewega-de Vriesa v teorii dlennykh voln. *MGI* **1**, 19 (1974).
14. C. C. Mei and B. Le Mehaute, Note on the equations of long waves over an uneven bottom. *J. Geophys. Res.* **71**, 393 (1966).
15. A. A. Dorfman, *O neustanovivshikhsia dlennykh koltsevykh volnakh konechnoi amplitudy, vyzvannykh peremeshcheniami dna basseina*. V sb.: *Teoria Voln i Raschet Gidrotekhnicheskikh Sooruzheny*. Nauka, Moscow (1975).
16. A. A. Dorfman and G. I. Yagovdik, *Uravenia priblizhennoi nelineino-dispersionnoi teorii dlennykh gravitatsionnykh voln, vzbushdaemykh peremeshcheniami dna i rasprostranyayushikhsia v basseine peremennoi glubiny*. V sb.: *Chislennyye Metody Mekhaniki Sploshnoi Sredy*. Vol. 8, p. 36, Novosibirsk (1977).
17. R. R. Long, The initial value problem for long waves of finite amplitude. *J. Fluid Mech.* **29**, 161 (1964).
18. V. F. Ivanov and L. V. Cherkosov, *O roli sovmestnogo efekta dispersii i nelineinosti pri dvizhenii voln tsunami v shelfovoi zone*. V sb.: *Teoria i Operativny Prognoz Tsunami*, p. 18, Nauka, Moscow (1980).
19. J. L. Bonna and R. Smith, A model for the two-way propagation of water waves in a channel. *Math. Proc. Camb. Phil. Soc.* **79**, 167 (1976).
20. B. L. Rozhdestvensky and N. N. Yanenko, *Sistemy Quasi-Lineinykh Uravneny i Ikh Prilozhenia k Gazovoi Dinamike*, p. 687, Nauka, Moscow (1978).
21. S. K. Godunov and V. S. Ryabenky, *Raznostnie skhemy (vvedenie v teoriiu)*, p. 400, Nauka, Moscow (1973).
22. M. I. Zhelezniak, *K Chislennomu Raschetu Vstrechnykh Vzaimodeistvy Poverkhnostnykh Voln*, Vol. 39, p. 44, Gidromekhanika, Kiev (1979).
23. Yu. I. Shokin, *Metod Differentsialnogo Priblizhenia*, p. 222, Nauka (1979).
24. B. Engquist and A. Majda, Absorbing boundary conditions for the numerical simulation of waves. *Maths Comput.* **31**, 629 (1977).
25. L. V. Cherkosov, *Gidrodinamika voln.*, p. 364, Nauka dumka, Kiev (1980). 364 s.